

11.11.80 А2

**ОБЪЕДИНЕННЫЙ  
ИНСТИТУТ  
ЯДЕРНЫХ  
ИССЛЕДОВАНИЙ  
ДУБНА**

**E1-84-278**

**A.P.Gasparian, N.S.Grigalashvili\***

**ANOMALOUS CARBON NUCLEI**

Submitted to "Zeitschrift für Physik"

---

\* On leave from Institute of High Energy Physics,  
Tbilisi, USSR

---

**1984**

---

## 1. INTRODUCTION

Nowadays there is a relatively large amount of information<sup>/1-24/</sup> on anomalous interaction cross sections for multicharged spectator fragments of high energy nuclei. Experiments<sup>/1-11/</sup> have been performed using nuclear emulsions exposed to cosmic rays and  $^{16}\text{O}$ ,  $^{40}\text{Ar}$ ,  $^{56}\text{Fe}$  nuclear beams from the Berkeley accelerator at a kinetic energy of (1-2) GeV per nucleon of the projectile nucleus. The phenomenon means that at a few first centimeters after emerging from a nuclear interaction, the projectile fragments (PF) exhibit significantly larger cross sections than those expected. If this is assumed to be connected with the production of excited nuclear fragments, the corresponding lifetime becomes anomalously large,  $\tau_n \approx 10^{-10}$  sec.

Experiments<sup>/12, 13/</sup> have been also carried out using nuclear emulsions exposed to  $^{12}\text{C}$  and  $^{22}\text{Ne}$  from the Dubna accelerator at 4.1 GeV/c per nucleon. Experimental data<sup>/12/</sup> do not contradict an evidence for an anomalous increase in the cross section of fragments with charges  $2 \leq Z_f \leq 10$  over first several centimeters from their formation point. Using significantly larger statistics, the authors<sup>/13/</sup> rule out the existence of any anomalies for  $^{22}\text{Ne}$  fragments with  $3 \leq Z_f \leq 9$ .

Recently experimental data have been published<sup>/14-16/</sup> on a study of this phenomenon using CR-39 plastic track detectors in a beam of  $^{40}\text{Ar}$  nuclei at  $T_0 = 1.8$  GeV/A. The fragments with charges  $9 \leq Z_f \leq 15$  were analyzed. The obtained data confirm the nuclear emulsion results<sup>/1-12/</sup>. It should be noted<sup>/14-16/</sup> that a strange behaviour of the mean free path (MFP) of fragments,  $\lambda = \frac{1}{n\sigma}$ , was observed. The tendency to an anomalous decrease of  $\lambda$  was observed in two regions of distances from the formation point of fragments:  $x < 4$  cm and  $x > 4$  cm. In the vicinity of  $x \approx 4$  the MFP corresponds by the normal value. The search<sup>/17/</sup> for fractionally charged  $^{40}\text{Ar}$  fragments was also undertaken by the plastic track detectors. The result is negative.

The search<sup>/18/</sup> for singly charged anomalous was carried out by means of a deuterium bubble chamber exposed to deuterons at 7.9 GeV/c. The experimental data indicate no dependence of MFP on distance  $X$  for positive and negative particles.

Two electronic experiments<sup>/19, 20/</sup> have been undertaken to check the hypothesis of anomalon instability in a  $10^{-10}$ - $10^{-11}$  sec lifetime interval. In the first experiment<sup>/19/</sup> delayed  $\gamma$ -emission was searched for over an energy range of  $100 < \epsilon_\gamma < 2000$  MeV

in the rest system of fragment from  $^{56}\text{Fe}$  interactions with iron target at  $T_0 = 940$  MeV. Such high energies of  $\gamma$ -quanta correspond to very anomalous excitations of nuclei. The expected  $\gamma$ -emission was not found. The second experiment<sup>/20/</sup> was performed by bombarding alternatively solid (20 mm thick) and dilute (ten 2-mm slabs each separated by 20 mm) Cu targets with a beam of 1.7 GeV/c  $^{56}\text{Fe}$  ions. The produced projectile fragments were detected and analyzed within a  $+1^\circ$  opening angle cone 5.5 m downstream. The dependence of the ratio of fragment yields on the solid and dilute targets on their charge was investigated. No statistically reliable deviation of the ratios from unity was observed. The experimental data analysis leads to the following conclusion: if anomalous exist, their mean lifetime is  $\tau_a \geq 5 \cdot 10^{-11}$  sec.

Experimental investigations of the behaviour of cross sections for spectator PF are being performed<sup>/21-24/</sup> by the collaboration on a treatment of pictures taken from the 2 m propane ( $\text{C}_3\text{H}_8$ ) bubble chamber (LHE, JINR) exposed to a beam of carbon nuclei at 4.2 GeV/c per nucleon. An indication has been obtained of an enhanced cross section for interactions of fragments with charges  $Z_f = 5$  and 6 at distances of  $X \geq 10$  cm. The characteristics of  $\gamma$ -quanta accompanying the production of fragments with charges  $Z_f = 5$  and 6 were also studied. An excess was observed over the background of  $\gamma$ -quanta from  $\pi^0$ -meson decays for energies  $\epsilon_\gamma < 70$  MeV in the rest system of the fragments.

In the last few years a number of theoretical approaches has been suggested to explain this phenomenon both within the frame of collective excitement models of peculiar nuclear states<sup>/25-31/</sup> and models taking into account quark degrees of freedom in nuclei<sup>/32-42/</sup>. More detailed information on the theoretical models can be found in the review<sup>/43/</sup>.

## 2. EXPERIMENTAL DATA

In this paper primary attention is given to an investigation of the dependence of the mean free path of carbon fragments with charges  $Z_f = 5$  and 6 on the distance from their formation point. Only primary interactions of beam carbon are used as a source of fragments. Background particles in the beam do not exceed (3+1)% for the experimental material under study and consist of carbon fragments with  $Z_f \geq 4$ . The chamber was placed in the magnetic field with average  $B = 1.5$  tesla.

The effective volume of the chamber for primary stars was chosen so that the minimal potential length, on which interaction could occur, was equal to 30 cm. The tracks of the fragments were scanned on this length from the vertex of a primary

star to search for interactions observed visually. The distance from the primary vertex to the interaction point of a secondary fragment or to its leaving from the effective volume was measured within an accuracy of 0.1 cm. The charge of spectator fragments can be identified in the bubble chamber by the density of ionization losses. According to this criterion, doubly-charged fragments are reliably separated from singly- and multi-charged fragments with  $Z_f \geq 3$ . For the fragments with  $Z_f \geq 3$  ionization losses are so large that the possibility of individual separation of charges  $Z = 3, 4, 5, 6$  is mainly restricted. To identify these fragments, the criterion of  $\delta$ -electron densities on tracks can be used<sup>/44/</sup>. However, the number of  $\delta$ -electrons fluctuate according to the Poisson law, and over a small length of tracks it is practically impossible to reliably identify the fragment charge due to a small number of  $\delta$ -electrons.

In order to reduce methodical errors in identifying charges and visual separation of overlapped tracks and stars produced by different particles going out of the same primary collision, only low multiplicity peripheral interactions of beam carbon nucleus with propane were selected. Moreover, according to the charge conservation law, the topology of primary interactions was not in contradiction with the hypothesis of fragment charge  $Z_f = 5$  or 6.

In all, approximately 50 000 visually observed interactions of carbon with propane were scanned. Only five topologies of primary interactions were selected. In all the topologies one and only one multicharged fragment flying in the beam direction was required. The measurements have shown that the angular deviation of multicharged fragment to the beam direction does not exceed  $2^\circ$ . Moreover, the density of ionization losses and  $\delta$ -electrons should be visually changed slightly relative to the beam one. A description of the topologies under study is given below.

1) Two-prong stars. One track is a multicharged fragment. A second track is a proton-recoil identified by range and ionization density. In the propane chamber for carbon exposure, protons are well detected and identified at a momentum of  $180 \leq P_p \leq 700$  GeV/c. In some part of events, 5%, the proton-recoil flies off to the backward hemisphere in the laboratory system, which undoubtedly corresponds to the interaction with carbon. In this topology secondary fragments can be  $^{12}\text{C}$  nuclei and  $\beta^+$ -active isotopes  $^{11}\text{C}$  and  $^{10}\text{C}$ . The isotopes  $^{10}\text{C}$  and  $^{11}\text{C}$  can be formed in the interaction of neutrons of primary carbon with protons of target.

2) Two-prong stars. One track is a spectator fragment. A second one can be a  $\pi^+$ -meson, a proton with  $P_p \geq 0.7$  GeV/c, a deuteron with  $P_d \geq 1.5$  GeV/c and a triton with  $P_t \geq 2$  GeV/c. In other words, the second track, with the exception of  $\pi^+$ -meson,

should be a relativistic positive single-charged particle. In this topology secondary fragments can be  $^{11}\text{C}$  and  $^{10}\text{C}$  isotopes produced in the interaction of neutrons of beam carbon with protons of target and stable relative to the  $\beta$ -decay of isotopes  $^{11}\text{B}$  and  $^{10}\text{B}$ . If in the first topology secondary  $^{12}\text{C}$  nuclei can be formed due to elastic scattering on proton or inelastic interaction with carbon of target, in the second topology such a possibility is practically unrealizable.

3) Three-prong stars. Except a multicharged fragment, there is one relativistic single-charged positive particle and a proton-recoil. In this case the  $^{11}\text{B}$  and  $^{10}\text{B}$  isotopes can be formed.

4) Three-prong stars. Besides one multicharged fragment, there is one positive single-charged particle with any energy and one negative particle,  $\pi^-$ -meson. At our energies the contribution of negative strange particles is smaller than 1%. In this topology the production of carbon isotopes  $^{11}\text{C}$  and  $^{10}\text{C}$  is mainly expected in the interaction of neutrons of beam carbon with neutrons of target.

5) Four-prong stars. Besides one multicharged fragment, there are two positive single-charged particles and one negative particle,  $\pi^-$ -meson. In this case  $^{11}\text{C}$ ,  $^{10}\text{C}$ ,  $^{11}\text{B}$ , and  $^{10}\text{B}$  isotopes can be formed. Thus, in the events selected the charge of investigated fragments was fixed with the topology of carbon primary interaction itself, and ionization losses did not contradict its expected value. It should be noted that the events of topologies 4 and 5 were selected from the part of the material of  $\approx 30\,000$  primary interactions. All topologies of the selected events on secondary charged particles accompanying the multicharged fragment are like NN interactions:

$$\begin{aligned}
 np &\rightarrow (+) X^0 \\
 pn &\rightarrow (+) X^0 \\
 pp &\rightarrow (++) X^0 \\
 nn &\rightarrow (+-) X^0 \\
 np &\rightarrow (++) X^0 \\
 pn &\rightarrow (++) X^0
 \end{aligned}
 \tag{1}$$

here  $X^0$  corresponds to a neutral component which can consist of neutrons and  $\pi^0$ -mesons. Let us note once more that collisions with  $^{12}\text{C}$  nucleus conservation belong to the first topology.

In Table 1 is shown statistics of the selected events according to the topologies. For topologies 4 and 5 the numbers of events normalized to 50 000 primary interactions are equal to 280 and 1030, respectively. Figure 1 presents the dependence of the number of noninteracting fragments with  $Z_f = 5$  and 6 on

Table 1

Number of events with the production of fragments with charges  $Z_f = 5$  and 6 according to the topologies. Topologies 4 and 5 were selected on some part of the experimental material (see text)

| Topology         | 1    | 2    | 3    | 4   | 5   | $\Sigma$ |
|------------------|------|------|------|-----|-----|----------|
| Number of events | 2168 | 1197 | 1580 | 170 | 616 | 5731     |

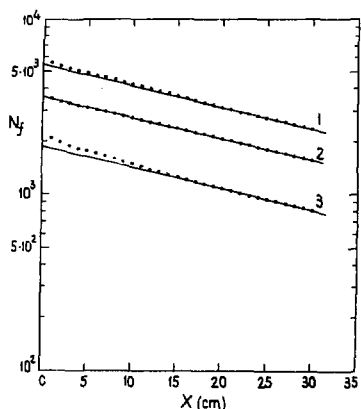


Fig.1. Dependence of the number of noninteracting fragments with  $Z_f = 5$  and 6 on the distance  $X$  from the primary star. The solid line corresponds to the expected attenuation of fragments.

the distance  $X$  from the primary star. The upper points (1) correspond to attenuation for all fragments with  $Z_f = 5$  and 6, taking all the topologies together. The middle points (2) correspond to the fragments found in topologies 2-5. The lower points (3) correspond to the fragments found in the first topology. The attenuation is presented for the fragments which did not interact at a first centimeter, i.e., the events with interaction at (0-1) cm distances were excluded from our analysis. This is connected with methodical difficulties. The possibility of spatial resolution of primary and secondary interactions, evaluation of ionization losses and definition of topology is lost with decreasing distance  $X$ . The expected attenuation of fragments normalized to the number of fragments which have escaped interaction at a distance of  $X = 20$  cm is shown in fig.1 by solid lines. The expected attenuation was calculated using the previously measured <sup>45/</sup> cross section of visually observed stars from the interactions of beam carbon nuclei with propane. The appropriate MFP <sup>45/</sup> is equal to  $\lambda_c = (35.68 \pm 0.45)$  cm.

From Fig.1 it is distinctly seen that the anomaly is observed for fragments with  $Z_f = 6$  from the first topology. The analysis of each topology separately has shown that there are no

Table 2

Dependence of the mean free path, MFP, for fragments of the first and other topologies together on distance X

| X(cm)  | 1-7          | 7-14       | 14-21      | 21-30      |
|--------|--------------|------------|------------|------------|
| first  | 24.93 ± 1.18 | 28.44±1.50 | 32.49±2.05 | 36.0±2.54  |
| others | 35.27 ± 1.50 | 36.38±1.60 | 35.74±1.71 | 36.44±1.74 |

Table 3

Dependence of the mean free path, MFP, for fragments of the first and other topologies together on distance X

| X(cm)  | 1-4   | 4-7   | 7-10  | 10-13 | 13-16 | 16-19 | 19-22 | 22-26 | 26-30 |
|--------|-------|-------|-------|-------|-------|-------|-------|-------|-------|
| first  | 21.53 | 23.60 | 28.29 | 27.96 | 32.08 | 34.18 | 31.50 | 36.11 | 36.07 |
|        | ±1.30 | ±2.23 | ±2.20 | ±2.27 | ±2.94 | ±3.38 | ±3.13 | ±3.51 | ±3.70 |
| others | 33.58 | 37.13 | 37.40 | 36.21 | 35.42 | 35.29 | 33.40 | 36.90 | 38.36 |
|        | ±1.94 | ±2.35 | ±2.46 | ±2.45 | ±2.47 | ±2.57 | ±2.47 | ±2.61 | ±2.92 |

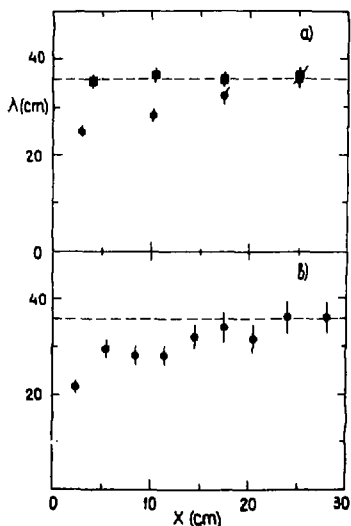


Fig.2. Dependence of the mean free path, MFP, for fragments on the distance X for the first topology (circles) and other topologies together (squares). The dashed line corresponds to the MFP for beam nuclei of carbon.

appreciable anomalies for fragments with  $Z_f = 5$  and 6 from topologies (2-5). Figure 2 and Tables 2 and 3 show the dependence of MFP for fragments on the distance X for the first topology (circles) and the other topologies together (squares). Potential distance X was divided into a number of segments  $\Delta X$ . For each segment the number of interactions N over length  $X_i \leq X \leq X_i + \Delta X$  and the number of noninteracting fragments  $N_0$  over length  $X_i \geq X \geq 1$  cm, flux, were counted. The mean free path was determined according to the

formula

$$N = N_0 [1 - \exp(-\frac{\Delta X}{\lambda})], \quad (2)$$

with  $\Delta X$  the length of an  $i$ -th segment, thickness of target;  $\lambda$  is an unknown path. A dashed line corresponds to the MFP for beam carbon nuclei.

So significant deviations from the expected dependence are not explained by statistical fluctuations. For instance, the data of fig.2a (circles) correspond to  $\chi^2/N.D.F. = 24.01$ .

Approximating the experimental points of fig.1 for fragments with  $Z_f = 6$  for the first topology as a sum of two exponentials, we get a (15+2)% contribution of anomalous carbon nuclei with  $\lambda_a = (6.46 \pm 1.81)$  cm. From the data of figs.1 and 2b one can see that for  $X \leq 5$  cm the value of MFP has a tendency to a sharper decrease.

In our experiment the overlapping of background tracks and stars produced by different fragments going out of the same primary interactions in a main danger because of a considerably worse spatial resolution as compared to nuclear emulsions. Moreover, the methodical possibility to exclude the overlaps vanish with decreasing distance  $X$ . The spatial resolution for the material being studied is evaluated to be 0.7 mm. For these primary energies various charged fragments and neutrons of beam carbon nuclei fly in a narrow cone to the beam direction.

The mean free path of neutron for the production of visually observed stars in propane is equal to  $\approx 150$  cm. In order to estimate background events, the angular distribution for positively singly charged particles with  $P_{\perp} = 3$  GeV/c was taken as an angular distribution of neutrons. Assuming that one energetic neutron is produced in each primary collision, the contribution of background stars at a distance of  $X \leq 7$  cm is equal to (3+1)%. Table 4 presents the dependence of the number of interacting fragments on the distance  $X$  for the first topology. From these data the excess of stars for  $X \leq 7$  cm is estimated to be 40%. It is clear that such an excess cannot be explained by the interaction of neutrons accompanying the fragment under study.

The overlaps of charged particles were evaluated by analyzing various carbon interactions which could visually imitate the topology in question. Let us consider this procedure for the first topology. From some part of the material the events were selected which also had a proton recoil, but a  $\pm 4^\circ$  narrow forward cone contains 2-6 fragments. All the observed events were divided into 10 topologies in which the total charge of a jet of fragments was equal to six: (5 + 1), (4 + 2), (3 + 3), (4 + 1 + 1), (3 + 2 + 1), (2 + 2 + 2), (2 + 2 + 1 + 1), (3 + 2 + 1 + 1), (2 + 1 + 1 + 1 + 1) and (1 + 1 + 1 + 1 + 1 + 1). The topologies

Table 4

Number of interacting fragments versus distance X for  
the first topology

| X (cm) | 1-3   | 3-5   | 5-7   | 7-9   | 9-11  | 11-13 | 13-15 | 15-17 |
|--------|-------|-------|-------|-------|-------|-------|-------|-------|
| first  | 185   | 141   | 123   | 121   | 100   | 96    | 85    | 68    |
|        | 17-19 | 19-21 | 21-23 | 23-25 | 25-27 | 27-29 | 29-31 |       |
|        | 68    | 72    | 56    | 52    | 49    | 44    | 45    |       |

(2 + 2 + 2), (5 + 1) and (2 + 2 + 1 + 1) were the most probable ones. The change of the contribution of the topologies depending on opening angles of ( $+1^\circ$ ,  $+2^\circ$ ,  $+3^\circ$ ,  $+4^\circ$ ) was analyzed. Moreover, the total mean square charge of a jet of fragments  $\langle Z_j^2 \rangle = 16+1$  and the ratio of the mean cross section of the jet to the cross section of beam carbon  $R = 1.4+0.1$  were estimated. The values of  $\langle Z_j^2 \rangle$  and R were found to be weakly dependent on angular restrictions within  $\theta \leq 4^\circ$ .

If one of the particles of a jet interacts at small distances X, then this event can be taken as a true one. In other words, false events arise while even if one particle of a jet interacts. For the first topology the contribution of false background interactions in an interval of  $X \leq 7$  cm is estimated to be equal to (15+3)%. This estimate was done without taking into account ionization criterion which in some events allows one to exclude background interactions. We see that the overlappings of charged particles make a more significant contribution as compared to neutrons.

However, a similar analysis performed with the other topologies (2-5) has shown that such quantities as  $\langle Z_j^2 \rangle$ , R and relative contributions of false stars in an interval of  $X \leq 7$  cm were found to be approximately equal to the corresponding values for the first topology. So we had to observe the decrease of MFP for all the topologies if it is due to overlappings.

For independent estimation of the contribution of overlappings, we have also done an additional methodical analysis which is sensitive to the overlapping of charged particles at very small angles. Two spatially separated particles with charges  $Z_1$  and  $Z_2$  ionize proportionally to  $Z_1^2 + Z_2^2$ , whereas one particle with  $Z = Z_1 + Z_2$  ionizes in proportion to  $(Z_1 + Z_2)^2$ . These two cases by ionization losses can be greatly different. Two particles can ionize as a single whole only in the case when the distance between them is smaller than the atomic one  $\leq 10^{-8}$  cm.

Table 5

Normalized  $\delta$ -electron density versus distance  $X$  for the first and other topologies and for all the observed fragments

| $X(\text{cm})$ | 1-7               | 7-14              | 14-21             | 21-30             |
|----------------|-------------------|-------------------|-------------------|-------------------|
| first          | $1.000 \pm 0.046$ | $0.96 \pm 0.04$   | $1.01 \pm 0.03$   | $0.990 \pm 0.015$ |
| others         | $0.720 \pm 0.036$ | $0.810 \pm 0.025$ | $0.790 \pm 0.023$ | $0.820 \pm 0.015$ |
| all            | $0.84 \pm 0.03$   | $0.86 \pm 0.02$   | $0.88 \pm 0.02$   | $0.88 \pm 0.01$   |

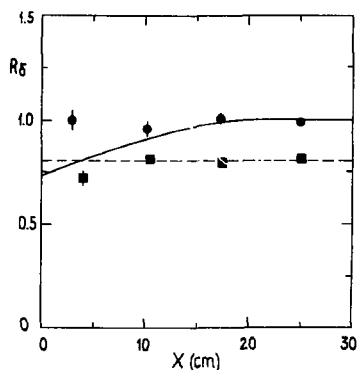


Fig.3. Normalized  $\delta$ -electron density dependence on the distance  $X$  for the first topology (circles) and for the others together (squares).

Such a system will strongly interact as two independent particles and electromagnetically as an entire particle. This phenomenon is possible for the fragmentation of nuclei too but only at gigantic primary energies when the opening angle of fragments is negligibly small.

For the fragments under investigation measurements of  $\delta$ -electron density were performed<sup>/44/</sup>. For each topology the  $\delta$ -electron density on beam carbon was determined, which was used as a monitor. The count of  $\delta$ -electron on secondary fragments was done as well. All the fragments were classified into four groups depending on value  $X$ : (1-7) cm, (7-14) cm, (14-21) cm, and (21-30) cm. Figure 3 and Table 5 show the normalized  $\delta$ -electron density versus distance  $X$  for the first topology (circles) and for the others (squares). A solid line corresponds to the expected behaviour when an experimental excess of interactions (see Table 4) is assumed to be completely due to overlappings with  $\langle Z_j^2 \rangle = 16$ . A dashed line gives the mean value of  $R_\delta$  over all  $X$  for the other topologies.

It is seen that the experimental points (circles) are in good agreement with the expected value of  $R_\delta = 1(\chi^2/\text{N.D.F.} = 0.39)$  which corresponds to the absence of overlappings. The analysis of the data of Table 5 leads to the conclusion that the contribution of overlappings is less than 10%.

So the methodical distortions are not able to explain all the set of experimental data.

The measurements of  $\delta$ -electron densities allow one to determine a charge contribution of fragments to the topologies. As expected, the first topology contains fragments with charge equal to beam carbon,  $Z_f = 6$ . In the other topologies together (2-5) there are fragments with  $Z_f = 6$  in 38% and with  $Z_f = 5$  in 62%. If all fragments are investigated without classification into topologies, experimental material will contain 59% fragments with  $Z_f = 6$  and 41% with  $Z_f = 5$ .

### 3. CONCLUSION

The dependence of the mean free path of projectile fragments has been investigated in a wide interval of distances from the point of their formation,  $1 \leq X \leq 30$  cm. The anomalous decrease of MFP is observed only for such primary interactions of beam nuclei  $^{12}\text{C}$  where carbon  $^{12}\text{C}$  can be formed as a secondary fragment. This follows from the analysis of all our experimental data. On the one hand, the fragments with  $Z_f = 6$  are often produced in other primary interactions, topologies (2-5). However, for these events no anomalies are observed. On the other hand, it is clear that nuclei  $^{12}\text{C}$  are not practically contained in these topologies. Here the fragments with  $Z_f = 6$  consist of  $^{11}\text{C}$  and  $^{10}\text{C}$  isotopes.

The number of secondary nuclei  $^{12}\text{C}$  can be estimated by comparing the numbers of events of the first and third topologies (see Table 1). According to our estimation, the first topology comprises approximately 600  $^{12}\text{C}$  nuclei. These nuclei can be formed in the interactions on target carbon with the emission of proton mainly in the forward hemisphere. Some part of nuclei  $^{12}\text{C}$  emerges due to elastic scattering on protons of target with  $P_{\perp} \geq 0.2$  GeV/c. The elastic scattering with such momentum transfer is about 10% of the total elastic scattering of carbon on proton. Half the  $^{12}\text{C}$  nuclei under study exhibits the anomalous decrease of MFP,  $\lambda_a = (6,46 \pm 1.8)$  cm. The tendency to a sharper decrease of  $\lambda_a$  at distances of  $X \leq 5$  cm is observed.

The main difficulties of this type of experiments is to change background conditions depending on the distance of a source of the fragments in question.

We are very indebted to the technical staff for film taking and to all members of the collaboration on film treatment from the 2m propane bubble chamber for their assistance in data processing. We are grateful to A.M.Baldin, M.I.Podgoretsky, M.I.Soloviev for variable discussions and notes, to H.N.Agakishiev, A.P.Cheplakov and M.Ya.Chubarian for their assistance in collecting and analyzing some of the data.

## REFERENCES

1. Milone A. Nuovo Cim.Suppl., 1954, 12, p.353.
2. Tokunaga S., Ishii T., Nishikawa K. Nuovo Cim., 1957, 5, p.517.
3. Yagoda H. Nuovo Cim., 1957, 6, p.559.
4. Friedlander E.M., Spirchez M. Nucl.Sci.Abstr., 1961, 15, p.347.
5. Judek B. Can.J.Phys., 1968, 46, p.343; 1972, 50, p.2082.
6. Cleghorn T.F., Freier P.S., Waddington C.J. Can.J.Phys. Suppl., 1968, 46, p.572.
7. Friedlander E.M. et al. Phys.Rev.Lett., 1980, 45, p.1084.
8. Jain P.L., Das G. Phys.Rev.Lett., 1982, 48, p.305.
9. Barber H.B., Freier P.S., Waddington C.J. Phys.Rev.Lett., 1982, 48, p.856.
10. Aggarwal M.M. et al. Phys.Lett.B, 1982, 112, p.31.
11. Friedlander E.M. et al. Phys.Rev.C, 1983, 27, p.1483.
12. Alekseeva E.A. et al. JETP Lett., 1983, 38, p.411.
13. Bannik B.P. et al. Proc. of the XVIII Int.Conf. on Cosmic Rays. India, August, 1983.
14. Tincknell M.L., Price P.B., Perlmutter S. Phys.Rev.Lett., 1983, 51, p.1948.
15. Heinrich W. et al. Nucl.Phys.A, 1983, 400, p.315c; Preprint Si-83-22, Siegen, 1983.
16. Drechsel H. et al. Preprint Si-83-14, Siegen, 1983.
17. Price P.B. et al. Phys.Rev.Lett., 1983, 50, p.556.
18. Clarke R.L. et al. Phys.Rev.D, 1983, 27, p.2773.
19. Liss T.M. et al. Phys.Rev.Lett., 1982, 49, p.775.
20. Gustafsson H.A. et al. Phys.Rev.Lett., 1983, 51, p.363.
21. Agakishiev H.N. et al. JINR, P1-81-79, Dubna, 1981; JINR, P1-82-795, Dubna, 1982.
22. Agakishiev H.N. et al. Z.Phys.C - Particles and Fields, 1983, 16, p.307.
23. Gasparian A.P., Grigalashvili N.S. Proc. of the Int.Conf. on Nucleus-Nucleus Collisions. Italy, August, 1983.
24. Agakishiev H.N. et al. Yad.Fiz., 1983, 38, p.999.
25. Hodel V. JETP Lett., 1982, 36, p.265.
26. Bayman B.F., Ellis P.J., Tang Y.C. Phys.Rev.Lett., 1982, 49, p.532.
27. Digiacomo N.J. Phys.Rev.Lett., 1982, 49, p.1593.
28. MacGregor M.H. Phys.Rev.Lett., 1982, 49, p.1815; Phys. Rev.C, 1983, 28, p.105.
29. Pshenin E.S., Voinov V.G. Phys.Lett.B, 1983, 128, p.133.
30. Karant Y.J., MacGregor M.H. Phys.Rev.Lett., 1983, 50, p.215.
31. McHarris Wm.C., Rasmussen J.O. Phys.Lett.B, 1983, p.49.
32. De Rujula A. et al. Phys.Rev.D, 1978, 17, p.285.
33. Karant Y.J. LBL Report, LBL-9171, Berkeley, 1979.

34. Romo W.J., Watson R.J.S. Phys.Lett.B, 1979, 88, p.354.
35. Stöcker H. et al. Phys.Lett.B, 1980, 95, p.192.
36. Slansky R. et al. Phys.Rev.Lett., 1981, 47, p.887.
37. Strikman M.I. Phys.Lett.B, 1981, 105, p.230.
38. Chapline G.F. Phys.Rev.D, 1982, 25, p.911.
39. Baym G. Prog.Part.Phys., 1982, 8, p.73.
40. Fredrikson S., Jändel M. Phys.Rev.Lett., 1982, 48, p.14.
41. Arbuzov B.A. JETP Lett., 1983, 37, p.403.
42. Arbuzov B.A., Baikov V.A., Boos E.E. Preprint ITEP 83-195, Serpukhov, 1983.
43. Karmanov V.A. UPhN, 1983, 141, p.525.
44. Gasparian A.P., Grigalashvili N.S. JINR, 1-11335, Dubna, 1979.
45. Akhababian N. et al. JINR, 1-12114, Dubna, 1979.

Received by Publishing Department  
on April 24, 1984.

Гаспарян А.П., Григалашвили Н.С.  
Аномальные ядра углерода

EI-84-278

Проведена обработка 50000 взаимодействий ядер углерода  $^{12}\text{C}$  в 2-метровой пропановой камере при первичном импульсе 4,2 ГэВ/с на нуклон. Подробно анализируются около 6000 пучковых фрагментов с зарядами  $Z_f = 5$  и 6 с целью выявления аномального уменьшения среднего свободного пробега /ССП/ фрагментов. Аномалия наблюдается только для вторичных ядер углерода  $^{12}\text{C}$ .

Работа выполнена в Лаборатории высоких энергий ОИЯИ.

Препринт Объединенного института ядерных исследований. Дубна 1984

Gasparian A.P., Grigalashvili N.S.  
Anomalous Carbon Nuclei

EI-84-278

Results are presented from a bubble chamber experiment to search for anomalous mean free path (MFP) phenomena for secondary multicharged fragments ( $Z_f = 5$  and 6) of the beam carbon nucleus at 4.2 GeV/c per nucleon. A total of 50000 primary interactions of carbon with propane ( $\text{C}_3\text{H}_8$ ) were treated. Approximately 6000 beam fragments with charges  $Z_f = 5$  and 6 were analyzed in detail to find out an anomalous decrease of MFP. The anomaly is observed only for secondary  $^{12}\text{C}$  nuclei.

The investigation has been performed at the Laboratory of High Energies, JINR.

Preprint of the Joint Institute for Nuclear Research. Dubna 1984

16 коп.

Редактор Э.В.Ивашевич. Макет Р.Д.Фоминой.  
Набор В.С.Румянцевой, И.Г.Андреевой.

Подписано в печать 10.05.84.  
Формат 60x90/16. Обетная печать. Уч. изд. листов 1,08.  
Тираж 485. Заказ 34645.

Издательский отдел Объединенного института ядерных исследований.  
Дубна Московской области.